Available online at www.sciencedirect.com
ScienceDirect
Ceramics International 35 (2009) 1407–1413
CERAMICS INTERNATIONAL
www.elsevier.com/locate/ceramint

Processing of dense nanostructured HAP ceramics by sintering and hot pressing

Dj. Veljović [a], B. Jokić [a], R. Petrović [a], E. Palcevskis [b], A. Dindune [b], I.N. Mihailescu [c], Dj. Janaćković [a,*]

[a] Faculty of Technology and Metallurgy, University of Belgrade, Karnegijeva 4, 11120 Belgrade, Serbia
[b] Institute of Inorganic Chemistry, Riga Technical University, Miera 34, Salaspils LV-2169, Riga, Latvia
[c] National Institute for Laser, Plasma and Radiation Physics, P.O. Box MG 36, 77125 Bucharest, Romania

Received 21 November 2007; received in revised form 17 June 2008; accepted 16 July 2008
Available online 5 August 2008

Abstract

A nanosized HAP powder was sintered and hot pressed, in order to obtain dense HAP ceramics. In a first series of experiments, the powder was isostatically pressed into uniform green compacts and sintered at temperatures ranging from 1000 °C to 1200 °C in air atmosphere for different times. In a second series, the isostatically pressed green compacts were hot pressed in argon atmosphere at 900 °C, 950 °C and 1000 °C. The SEM micrograph of the sample sintered at 1200 °C for 2 h showed a uniform 3 μm mean grain size dense microstructure. In the case of hot pressed HAP compacts, full dense, translucent nanostructures were obtained having mean grain size below 100 nm and improved mechanical properties. With the grain size decreasing from 3 μm to 50 nm, the fracture toughness of pure HAP ceramics increased from 0.28 MPa $m^{1/2}$ to 1.52 MPa $m^{1/2}$.

Keywords: A. Sintering; B. Grain size; C. Mechanical properties; D. Apatite

1. Introduction

Calcium hydroxyapatite, $Ca_{10}(PO_4)_6(OH)_2$, which is structurally similar to bone and tooth mineral, can adhere to, and integrate with, both bone and soft tissue well [1]. A large number of studies focused on conditions to get a HAP form suitable for incorporation in the living bone. Calcium hydroxyapatite in a dense sintered form is often used as a bioactive, biocompatible ceramic material in bone reparation [2,3]. This particular HAP is clinically very important for tooth root replacement, augmentation of alveolar ridges, pulp capping and maxillofacial reconstruction, among many others [4].

Sintering of HAP is a complex process since many parameters influence the sintering process. Given its poor sinterability, HAP ceramics shows low strength, especially in wet environments as would be found in physiological conditions [5]. Obtaining full dense nanostructures is the key to enhance the mechanical and biological properties of HAP-based bioceramic materials [6].

The mechanical properties and microstructures of the resulting HAP ceramics strictly depend on the characteristics of the original HAP powder, including crystallinity [7], agglomeration [8], stoichiometry, and substitutions [9], and on the processing conditions [10]. The different methods for obtaining nanosized HAP powder include solid-state reaction [11], ultrasonic spray-pyrolysis [12], sol–gel synthesis [13], catalytic decomposition of urea with urease [14], hydrothermal decomposition of urea, calcium–EDTA chelates [15], modified chemical precipitation, etc.

Due to their metastability, the nanosized powders are frequently agglomerated as a consequence of the high surface energy. Synthesis of agglomerate-free and soft agglomerated HAP nanostructured powders can be an important step toward making dense nanostructure materials with good mechanical properties. Removing the interagglomerate pores, responsible for poor sintering behavior, is the most common problem need to be solved in sintering of agglomerated nanopowders.

Nanostructured ceramics are usually processed by compacting nanopowders at high pressures and sintering at different

* Corresponding author. Tel.: +381 11 3370489; fax: +381 11 3370387.
E-mail address: nht@tmf.bg.ac.yu (D. Janaćković).

0272-8842/$34.00
doi:10.1016/j.ceramint.2008.07.007

times and temperatures and in various atmospheres. Pressure assisted methods, such as hot pressing, hot isostatic pressing, sinter forging, etc., are also applied to obtain nanostructured ceramic materials [16–18]. Hot pressing makes it possible to enhance densification kinetics and limit grain growth. This technique has been used to process HAP ceramics with a controlled microstructure.

During sintering and hot pressing, the calcium deficient apatite turns into a mixture of HAP and β-TCP. A high amount of β-TCP is highly detrimental to the sintering and mechanical properties of HAP bioceramics [19]. In order to avoid degradation of the mechanical properties, the absence of the β-TCP in HAP bioceramics is advisable. More investigation concerning the sintering of calcium phosphates is required in order to obtain dense or microporous bioceramics based on HAP [9,16,20,21]. Dense bioceramic materials made of HAP are either opaque white, or translucent.

The aims of this work were the processing and characterization of dense nanostructured HAP ceramics, obtained by sintering and hot pressing of nanosized HAP powder, as well as comparing the microstructural and mechanical properties of dense materials obtained by these two methods. Effects of grain size on microhardness and indentation fracture toughness of HAP ceramic materials were also investigated.

2. Experimental

A nanosized HAP powder was obtained using a modified chemical precipitation method, by the reaction of calcium oxide (obtained by calcination of $CaCO_3$ for 5 h at 1000 °C in air) and phosphoric acid [22–24]. Small portions of the resulting calcium oxide were mixed and stirred with distilled water for 10 min. The resulting calcium hydroxide suspension was poured through a sieve into the reaction vessel while simultaneously stirring and filtering to avoid unreacted CaO grains. A calculated amount of diluted 85% (1:1) phosphoric acid was added drop-wise to the calcium hydroxide suspension in accordance with the reaction:

$$10Ca(OH)_2 + 6H_3PO_4 \rightarrow Ca_{10}(PO_4)_6(OH)_2 + 18H_2O$$

The pH value of the reaction medium (∼10–11 at the beginning of synthesis) was kept under constant control throughout the synthesis process. When all the necessary quantity of phosphoric acid was introduced pH reached the value 7.4–7.6. The obtained suspension was heated to 94 ± 1 °C for 30 min and stirred for another 30 min. After sedimentation, the upper clear solution layer was detached. The suspension was then spray dried at 120 ± 5 °C into granulated powder.

Powder morphology and particle size were evaluated using a transmission electron microscope (Philips EM400) and scanning electron microscope (Jeol T-20). The specific surface area measurement was done using a BET surface area analysis. The nanopowders were checked for phase identification using X-ray diffraction (XRD) and FTIR analyses.

The synthesized HAP powder was isostatically pressed at 400 MPa, for 1 min, resulting into uniform green compacts, which were sintered at temperatures from 1000 °C to 1200 °C in air atmosphere for times ranging from 45 min to 8 h. The initial heating rate was 20 °C/min.

In other experiments, isostatically pressed green compacts were hot pressed at 20 MPa in argon atmosphere, at temperatures from 900 °C, 950 °C and 1000 °C, for various times from 1 h to 2 h.

The morphology of the pressed and sintered compacts was examined with a scanning electron microscope Jeol T-20, and Jeol JSM-6460LV was used to determine the morphology of the hot pressed compacts. The average grain size of the samples was determined by measuring the pulled out grains from the fracture surfaces of the materials, and evaluated by image analysis of SEM micrographs, using software for image analysis, Image Pro Plus Program, Version 4.0 for windows. More than 100 HAP grains were counted to obtain an average value. FTIR analyses of the HAP powder and the sintered and hot pressed compacts were performed using an MB Bomen 100 Hartmann and Braun spectrometer in the wavenumber range from 400 cm^{-1} to 4000 cm^{-1}. The samples were prepared by the KBr method at a sample ratio KBr = 1:150. X-ray diffraction analyses of HAP powder, sintered and hot pressed compacts were performed using the Philips PW1710 diffractometer with Cu Kα radiation and a graphite monochromator, with the angle 2θ ranging from 20° to 50° and the step scan of 0.02°. HAP compact density was measured using Archimedes' method. The sintered HAP compacts were tested for microhardness and indentation fracture toughness. Microhardness was measured with a Vicker's indenter. K_{IC} values were calculated using the following formula which was derived from the model proposed by Evans and Charles [25]:

$$K_{IC} = 0.0824Pc^{-3/2}$$

where P is the indentation load and c the length of the induced radial crack.

3. Results and discussion

The SEM micrograph of the obtained HAP powder is shown in Fig. 1. The HAP powder looks agglomerated and consists of

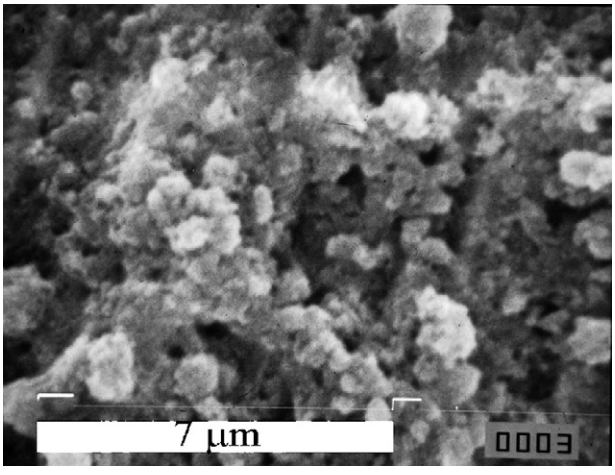

Fig. 1. Typical SEM micrograph of the HAP powder.

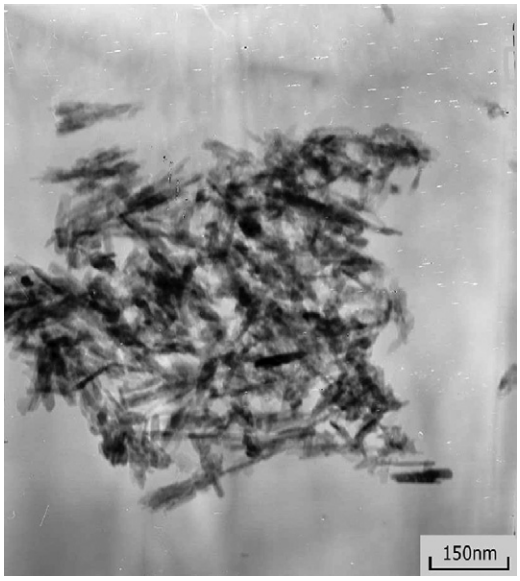

Fig. 2. TEM photograph of the HAP powder.

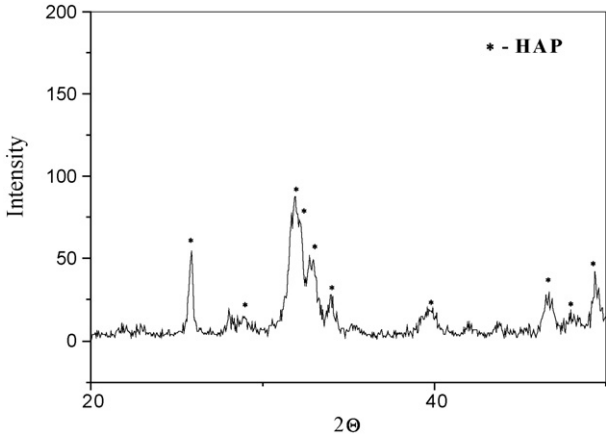

Fig. 3. XRD pattern of HAP powder.

large numbers of fine HAP particles. The TEM image of the resulting nanopowder shows the agglomerate which consist of nanosized rod-shaped particles 50–100 nm in size (Fig. 2).

The Ca/P ratio of the HAP powder, as determined by ICP analyses, was 1.67 ± 0.01. The specific surface area, determined by the BET method, was $59 \pm 5\ m^2/g$. The XRD pattern of the powder showed a very low crystallinity (Fig. 3). The only peaks recognized were those corresponding to the calcium hydroxyapatite phase. All the peaks perfectly matched the JCPDS pattern 9–432 for HAP, suggesting that pure HAP was obtained.

The Fourier transform infra-red (FTIR) analysis of the HAP powder (Fig. 4) revealed the characteristic bands corresponding to calcium hydroxyapatite: the phosphate group bands at 462 cm^{-1}, 553 cm^{-1}, 595 cm^{-1}, 958 cm^{-1}, and 1024–1115 cm^{-1}, the OH^- group band at 3584 cm^{-1} and 636 cm^{-1} and the HPO_4^{2-} band at 873 cm^{-1} [26].

The SEM micrograph of the green compact isostatically pressed at 400 MPa is shown in Fig. 5. The compact, as can be

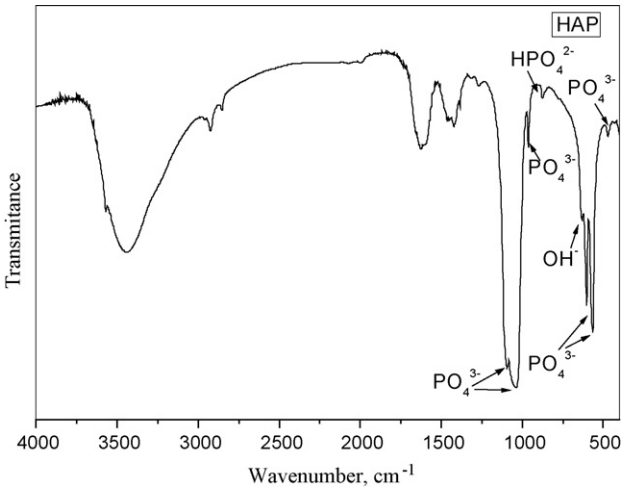

Fig. 4. FTIR spectra of HAP powder.

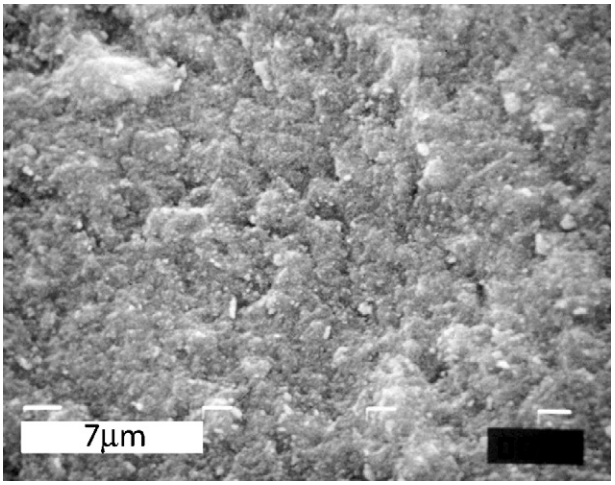

Fig. 5. Typical SEM micrograph of a green compact of HAP powder pressed at 400 MPa.

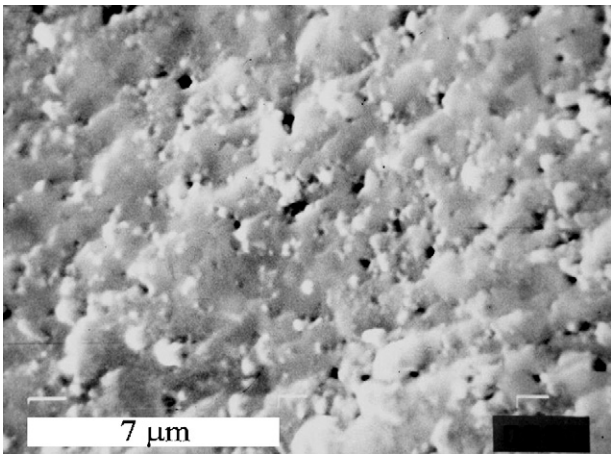

Fig. 6. SEM micrograph of a sample sintered at 1000 °C for 8 h (fracture surface).

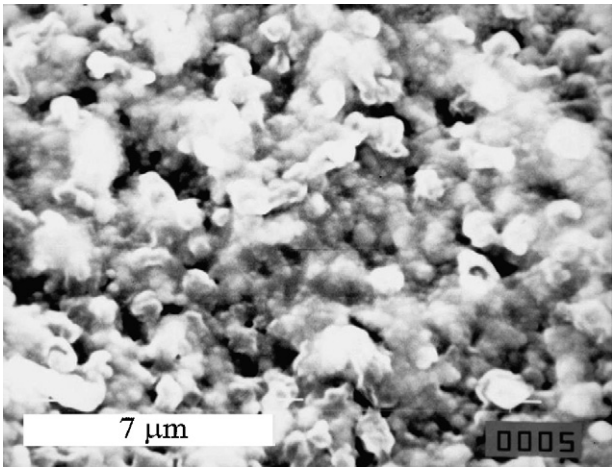

Fig. 7. SEM micrograph of a sample sintered at 1050 °C for 45 min (fracture surface).

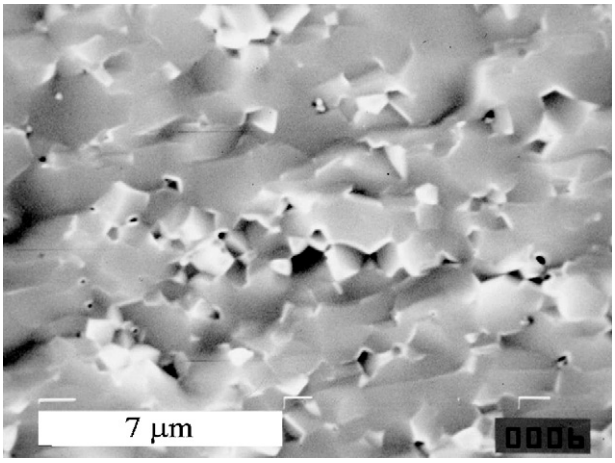

Fig. 8. SEM micrograph of a sample sintered at 1050 °C for 2 h (fracture surface).

clearly seen, was uniform, as the result of applied high isostatic pressure and the presence of soft aggregates in the starting HAP powder. The green compact density was 1.89 g/cm^3, or 60% of the theoretical density.

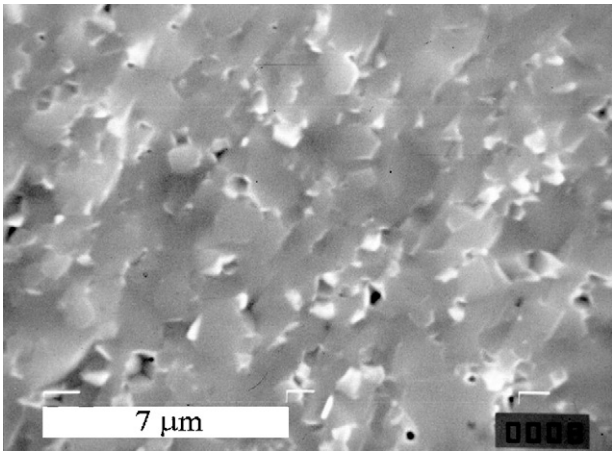

Fig. 9. SEM micrograph of a sample sintered at 1050 °C for 4 h (fracture surface).

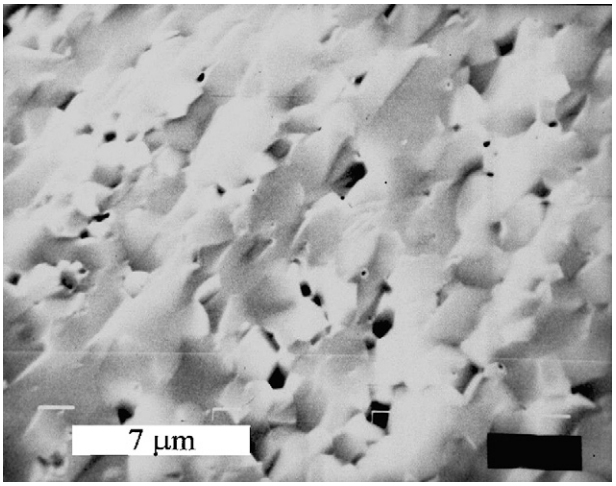

Fig. 10. SEM micrograph of a sample sintered at 1100 °C for 45 min (fracture surface).

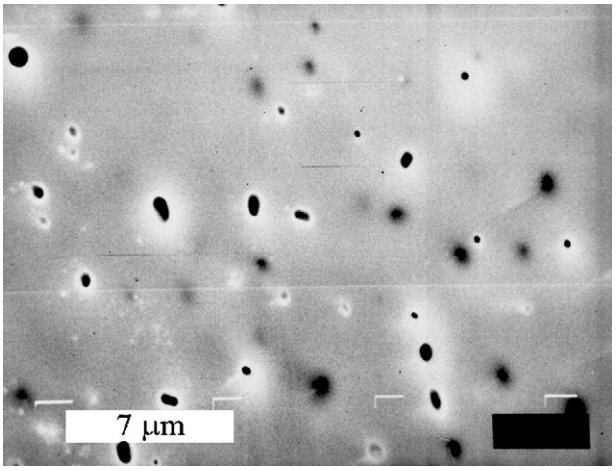

Fig. 11. SEM micrograph of a sample sintered at 1100 °C for 4 h (fracture surface).

In the first part of the experiment, green compacts of HAP were sintered in air to obtain compacts having a dense microstructure. The SEM micrograph of the fracture surface of a sample obtained by sintering at 1000 °C for 8 h is shown in Fig. 6. The figure shows that this compact has a porous microstructure with mean grain size of 300 nm. SEM micrographs of samples sintered at 1050 °C for 45 min, 2 h, and 4 h are shown in Figs. 7–9, respectively. The sample sintered at 1050 °C for 45 min had a high porosity, which decreased with increasing sintering time. On sintering in air at 1050 °C, the HAP compacts increased in grain size from 650 nm to 950 nm. The samples sintered at 1100 °C for 45 min (Fig. 10) and 4 h (Fig. 11) have a noticeable porosity as well. The SEM micrograph of the sample sintered at 1200 °C for 2 h showed a uniform dense microstructure with 3 μm mean grain size (Fig. 12).

In the second part of the experiments, green compacts were hot pressed at temperatures lower then 1000 °C, resulting in full dense HAP compacts with smaller grain size. The SEM micrographs of compacts hot pressed at 1000 °C for 2 h and 1 h

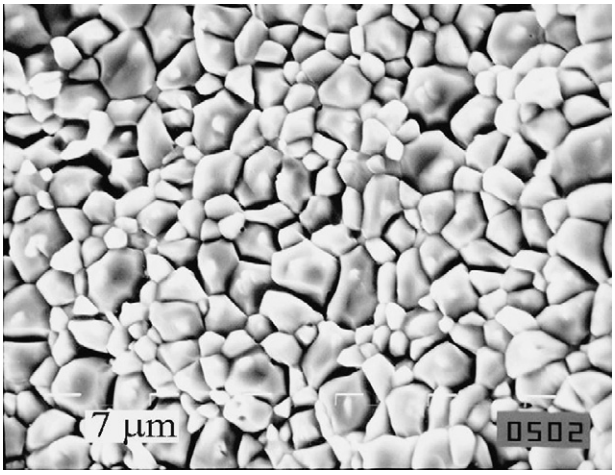

Fig. 12. SEM micrograph of a sample sintered at 1200 °C for 2 h (polished and etched).

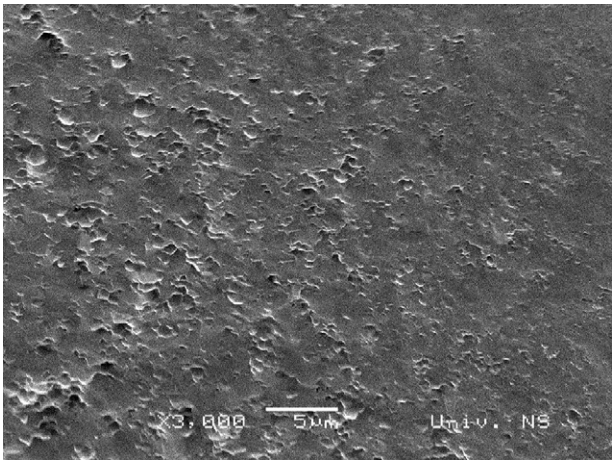

Fig. 13. SEM micrograph of a sample hot pressed at 1000 °C for 2 h (fracture surface).

are shown in Figs. 13 and 14, respectively. Both of these microstructures were nonporous, with mean grain sizes of 380 nm and 140 nm, and densities of 3.06 g/cm^3 and 2.99 g/cm^3, respectively. The mean grain size further decreased to

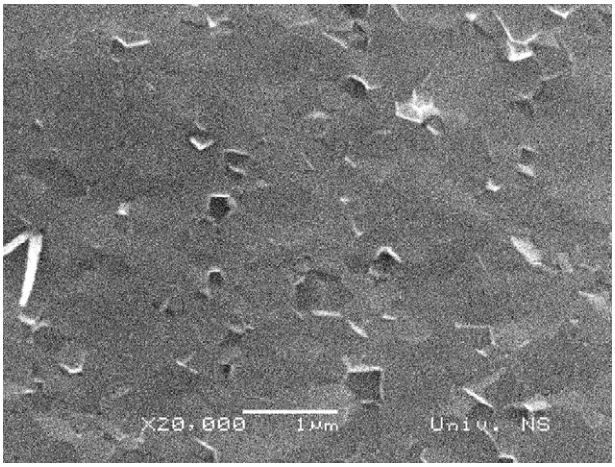

Fig. 14. SEM micrograph of a sample hot pressed at 1000 °C for 1 h (fracture surface).

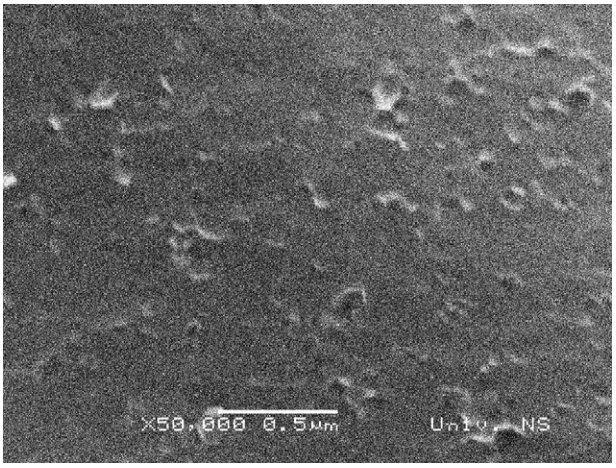

Fig. 15. SEM micrograph of a sample hot pressed at 950 °C for 2 h (fracture surface).

50 nm with decreasing hot pressing temperature to 950 °C (Fig. 15). The sample that was hot pressed at 900 °C for 2 h was porous (Fig. 16). The ceramics that reached full density were found to be translucent [1]. Hot-pressed dense nanostructured samples obtained at 1000 °C and 950 °C, were translucent.

The FTIR analysis of the samples sintered at 1200 °C for 2 h and hot pressed for 1 h at 1000 °C (Fig. 17) showed the characteristic bands corresponding to calcium hydroxyapatite.

The XRD pattern of a sample sintered at 1200 °C for 2 h and hot pressed at 1000 °C for 1 h (Fig. 18) showed peaks suggesting that HAP was the prevailing crystalline phase in the bioceramic materials obtained.

In a brittle ceramic material like HAP, the fracture toughness is very low, so after the critical load, the fracture surface generation processes consume more energy and the volume deformation process is left unchanged [27,28]. During the past decade, major advances have been made in developing ceramic microstructures, which increase the energy absorption during crack propagation [29]. Significant improvements have been made in fracture toughness increase of a polycrystalline ceramic through the control of density

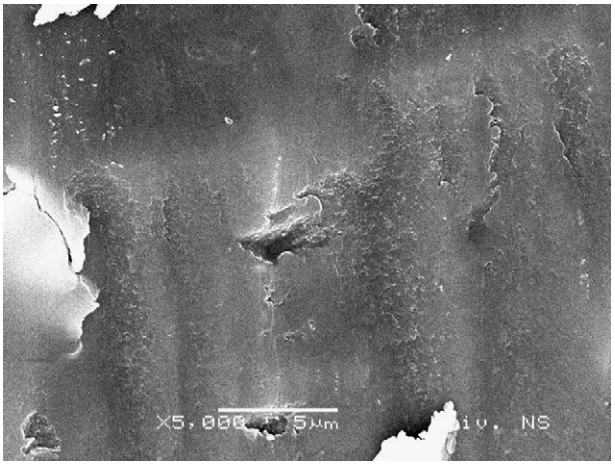

Fig. 16. SEM micrograph of a sample hot pressed at 900 °C for 2 h (fracture surface).

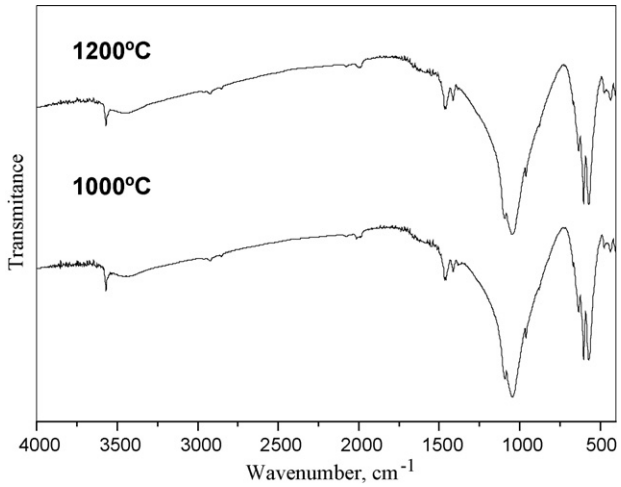

Fig. 17. FTIR spectra of samples sintered for 2 h at 1200 °C and hot pressed for 1 h at 1000 °C.

and microstructure characteristics, especially by effect of grain size [29–31].

The indentation fracture toughness of a compact hot pressed at 1000 °C for 1 h and of a compact sintered at 1200 °C for 2 h were determined by Vicker's indenter, to check the effect of grain size on fracture toughness. The fracture toughness as a function of grain size is showed in Fig. 19. It can be observed that with decreasing average grain size, fracture toughness of dense HAP ceramics significantly increases. The dense compact sintered at 1200 °C for 2 h has mean grain size of 3 μm, while fracture toughness was 0.28 MPa $m^{1/2}$. In dense compact hot pressed at 950 °C for 1 h, fracture toughness increased up to 1.52 MPa $m^{1/2}$ as the grain size decreased to 50 nm in average. This maximum value is slightly higher than the reported K_{IC} value of 0.88 MPa $m^{1/2}$ for HAP ceramics by Thangamania et al. [27] and Raynaud et al. [16] measured a fracture toughness of 1.0 ± 0.1 MPa $m^{1/2}$ in a hot pressed HAP/TCP ceramics with an average 200 nm grain size. Banerjee et al. [5] obtained dense HAP ceramics with lower fracture toughness ranging from 0.6 MPa $m^{1/2}$ to 1.0 MPa $m^{1/2}$.

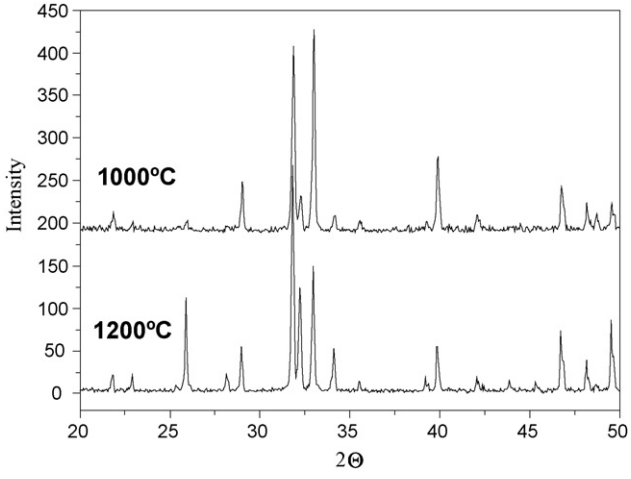

Fig. 18. XRD patterns of samples sintered for 2 h at 1200 °C and hot pressed for 1 h at 1000 °C.

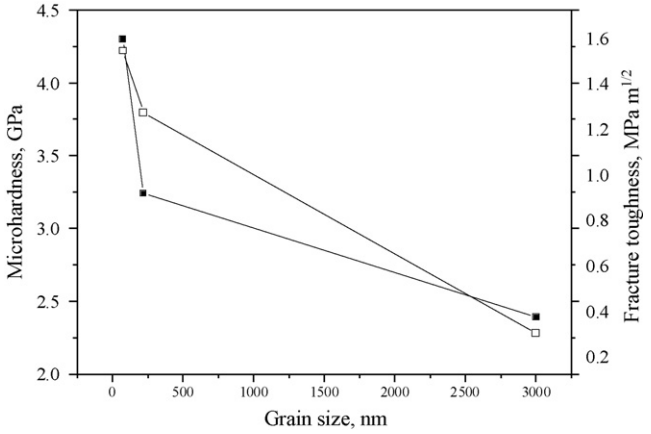

Fig. 19. Measured microhardness and fracture toughness as a function of grain size ((■), microhardness; (□), fracture toughness).

Transgranular and intergranular fractures are found in polycrystalline ceramic materials. The type of fracture is usually found to be transgranular in microstructured HAP ceramics, because the fracture cracks pass through the grains [27,32]. An increase of K_{IC} with decreasing grain size is usually observed in ceramics where fracture mechanism is intergranular because the major contribution to crack resistance is related to the crossing the cracks through the grain boundaries. With decrease in grain size, the part of the grain boundary phase is increased, and in that way the greater is energy absorption during crack propagation through the grained boundaries of such fine-grained microstructure (nanostructure).

In our case, Figs. 13 and 14 confirm the intergranular fracture mechanism in our nanostructured HAP ceramics (where the pulled out grains from the structure are observed). It could be supposed that decrease in grain size from micro to nano-level change the fracture mechanism from transgranular to intergranular, giving the explanation for the increasing of fracture toughness up to 1.52 MPa $m^{1/2}$.

The microhardness of the samples sintered at 1200 °C for 2 h and hot pressed at 1000 °C for 1 h and at 950 °C for 1 h was 2.39 GPa, 3.24 GPa and 4.30 GPa, respectively. The microhardness as a function of grain size is showed in Fig. 19. It can be observed that with decreasing of grain size, microhardness of dense HAP ceramics increases.

4. Conclusions

Dense HAP ceramics were produced by sintering and hot pressing of isostatically pressed green compacts. Air sintering at 1000 °C, 1050 °C, and 1100 °C resulted in compacts having porous microstructures. The SEM micrograph of the sample sintered at 1200 °C for 2 h shows a dense uniform microstructure with a average grain size of 3 μm. Hot pressing led to compacts with dense translucent nanostructures and average grain sizes ranging from 50 nm, for the sample hot pressed at 950 °C for 2 h to 380 nm, for the sample hot pressed at 1000 °C for 2 h. The XRD and FTIR analyses of the sintered and hot pressed samples revealed peaks and bands corresponding to the calcium hydroxyapatite phase, only. The mechanical properties

of the nanostructured HAP ceramics obtained by hot pressing were obviously better than those of the microstructured ceramics obtained by sintering in air. With the grain size decreasing from 3 μm to 50 nm, the fracture toughness of the dense HAP compacts increased from 0.28 MPa $m^{1/2}$ to 1.52 MPa $m^{1/2}$, while the microhardness increased from 2.39 GPa to 4.30 GPa.

Acknowledgements

The authors wish to acknowledge the financial support from Ministry of Science, Republic of Serbia through the projects 142070B and EUREKA E! 3033 Bionanocomposit.

References

[1] J.E. Barralet, G.J.P. Fleming, C. Campion, J.J. Harris, Formation of translucent hydroxyapatite ceramics by sintering in carbon dioxide atmospheres, J. Mater. Sci.: Mater. Med. 38 (2003) 3979–3993.
[2] L.L. Hench, Bioceramics: from concept to clinic, J. Am. Ceram. Soc. 74 (1991) 1487–1510.
[3] C. Kothapalli, M. Wei, A. Vasiliev, M.T. Shaw, Influence of temperature and concentration on the sintering behavior and mechanical properties of hydroxyapatite, Acta Mater. 52 (2004) 5655–5663.
[4] R.Z. Legeros, J.P. Legeros, Dense hydroxyapatite, in: L.L. Hench, J. Wilson (Eds.), An Introduction to Bioceramics, World Scientific, Singapore, 1993, pp. 139–180.
[5] A. Banerjee, A. Bandyopadhyay, S. Bose, Hydroxyapatite nanopowders: synthesis, densification and cell–materials interaction, Mater. Sci. Eng. C 27 (2007) 729–735.
[6] W.D. Kingery, H.K. Bowen, D.R. Uhlman, Introduction to Ceramics, John Wiley and Sons, New York, 1976, p. 808.
[7] E. Landi, A. Tampieri, G. Celotti, S. Sprio, Densification behaviour and mechanisms of synthetic hydroxyapatites, J. Eur. Ceram. Soc. 20 (2000) 2377–2387.
[8] M.G.S. Murray, J. Wang, C.B. Ponton, P.M. Marquis, An improvement in processing of hydroxyapatite ceramics, J. Mater. Sci. 30 (1995) 3061–3074.
[9] J.E. Barralet, S. Best, W. Bonfield, Effect of sintering parameters on the density and microstructure of carbonate hydroxyapatite, J. Mater. Sci.: Mater. Med. 11 (2000) 719–724.
[10] Dj. Veljovic, B. Jokic, I. Jankovic-Castvan, I. Smiciklas, R. Petrovic, Dj. Janackovic, Sintering behaviour of nanosized HAP powder, Key Eng. Mater. 330–332 (2007) 259–262.
[11] R.R. Rao, H.N. Roopa, T.S. Kanan, Solid state synthesis and thermal stability of HAP and HAP—β-TCP composite ceramic powders, J. Mater. Sci.: Mater. Med. 8 (1997) 511–518.
[12] M. Aizava, T. Hanazava, K. Itatani, F.S. Howell, A. Kishioka, Characterization of hydroxyapatite powders prepared by ultrasonic spray-pyrolysis technique, J. Mater. Sci. 34 (1999) 2865–2873.
[13] S. Bose, S.K. Saha, Synthesis of hydroxyapatite nanopowders via sucrose-templated sol–gel method, J. Am. Ceram. Soc. 86 (2003) 1055–1057.
[14] B. Jokic, D. Tanaskovic, I. Jankovic-Castvan, S. Drmanic, R. Petrovic, Dj. Janackovic, Synthesis of nanosized calcium-hydroxyaptite by the catalytic decomposition of urea with urease, J. Mater. Res. 22 (2007) 1156–1161.
[15] Dj. Janaćkovic, I. Petrović-Prelević, Lj. Kostić-Gvozdenović, R. Petrović, V. Jokanović, D. Usković, Influence of synthesis parameters on the particle sizes of nanostructured calcium–hydroxyapatite, Key Eng. Mater. 203 (2001) 192–195.
[16] S. Raynaud, E. Champion, J.P. Lafon, D. Bernache-Assollant, Calcium phosphate apatites with variable Ca/P atomic ratio III. Mechanical properties and degradation in solution of hot pressed ceramics, Biomaterials 23 (2002) 1081–1089.
[17] M.J. Mayo, Nanocrystalline ceramics for structural applications: processing and properties, in: G.M. Chow, N.I. Noskova, Nanostructured (Eds.), Materials Science and Technology, NATO ASI Series, Kluwer Academic Publishers, Russia, 1997, pp. 361–385.
[18] J.R. Groza, Nanosintering, Nanostruct. Mater. 12 (1999) 987–992.
[19] S. Raynaud, E. Champion, D. Bernache-Assollant, Calcium phosphate apatites with variable Ca/P atomic ratio II. Calcination and sintering, Biomaterials 23 (2002) 1073–1080.
[20] R.Z. Legeros, S. Lin, R. Rohanizadeh, D. Mijares, J.P. Legeros, Biphasic calcium phosphate bioceramics: preparation, properties and applications, J. Mater. Sci.: Mater. Med. 14 (2003) 201–209.
[21] F. Tancret, J.M. Bouler, J. Chamousset, L.M. Minois, Modelling the mechanical properties of microporous and macroporous biphasic calcium phosphate bioceramics, J. Eur. Ceram. Soc. 26 (2006) 3647–3656.
[22] M. Jarcho, C.H. Bolen, M.B. Thomas, J. Bobick, J.F. Kay, R.H. Doremus, Hydroxyapatite synthesis and characterisation in dense polycrystalline form, J. Mater. Sci. 11 (1976) 2027–2037.
[23] A. Osaka, Y. Miura, K. Takeuchi, M. Asada, K. Takahashi, Calcium apatite prepared from calcium hydroxide and orthophosphoric acid, J. Mater. Sci.: Mater. Med. 2 (1991) 51–55.
[24] E. Palcevskis, A. Dindune, L. Kuznecova, A. Lipe, Z. Kanepe, Granulated composite powders on basis of hydroxyapatite and plasma-processed zirconia and alumina nanopowders, Latvian J. Chem. 2 (2005) 128–138.
[25] A.G. Evans, E.A. Charles, Fracture toughness determinations by indentation, J. Am. Ceram. Soc. 59 (1976) 371–372.
[26] R.N. Panda, M.F. Hsieh, R.J. Chung, T.S. Chin, FTIR, XRD, SEM and solid state NMR investigations of carbonate-containing hydroxyapatite nano-particles synthesized by hydroxide-gel technique, J. Phys. Chem. Solids 64 (2003) 193–199.
[27] N. Thangamania, K. Chinnakalib, F.D. Gnanama, The effect of powder processing on densification, microstructure and mechanical properties of hydroxyapatite, Ceram. Int. 28 (2002) 355–362.
[28] B.R. Lawn, T. Jensen, A. Arora, Brittleness as an indentation size effect, J. Mater. Sci. Lett. 11 (1976) 573–575.
[29] Y.M. Chiang, D.P. Birnie, W.D. Kingery, Physical Ceramics, John Wiley and Sons, New York, 1997, pp. 477–485.
[30] B.R. Lawn, D.B. Marshall, Hardness, toughness and brittleness: an indentation analysis, J. Am. Ceram. Soc. 62 (1979) 347–350.
[31] P. van Landuyt, F. Li, J.P. Keustermans, J.M. Streydio, F. Delannay, E. Muting, The influence of high sintering temperatures on the mechanical properties of hydroxyapatite, J. Mater. Sci.: Mater. Med. 6 (1995) 8–13.
[32] W.D. Callister, Materials Science and Engineering An Introduction, John Wiley and Sons, New York, 2003, pp. 410–424.